

Zero-inflated stochastic volatility model for disaggregated inflation data with exact zeros

Geonhee Han*

Graduate School of Arts and Sciences, Columbia University

Kaoru Irie†

Faculty of Economics, The University of Tokyo

Feb 10 2025

Abstract

The disaggregated time-series data for Consumer Price Index (CPI) often exhibits frequent instances of exact zero price changes, stemming from measurement errors inherent in the data collection process. However, the currently prominent stochastic volatility model of trend inflation is designed for aggregate measures of price inflation, where exact zero price changes rarely occur. We formulate a zero-inflated stochastic volatility model applicable to such non-stationary real-valued multivariate time-series data with exact zeros. The Bayesian dynamic generalized linear model jointly specifies the dynamic zero-generating process. We construct an efficient custom Gibbs sampler, leveraging the Pólya-Gamma augmentation. Applying the model to disaggregated CPI data in four advanced economies — US, UK, Germany, and Japan — we find that the zero-inflated model provides more sensible and informative estimates of time-varying trend and volatility. Through an out-of-sample forecasting exercise, we find that the zero-inflated model delivers improved in point forecasts and better-calibrated interval forecasts, particularly when zero-inflation is prevalent.

Keywords: Bayesian, Zero-inflation, State-space model, Stochastic volatility, Disaggregate consumer price index

*420 W 118th St., New York, NY 10027, United States of America. gh2610@columbia.edu.

†7-3-1 Hongo, Bunkyo-ku, Tokyo, 113-0033, Japan. irie@e.u-tokyo.ac.jp

1 Introduction

In time series analysis, data are often transformed into first differences or rates of change to facilitate statistical modeling, inference, and prediction. A classic example is the Box–Jenkins autoregressive integrated moving average (ARIMA) framework (Box et al., 2015, Chap. 9), where trend and seasonal variations are removed by differencing; financial applications frequently define stock returns as the percentage change in stock prices between consecutive time points (Hautsch et al., 2013). The transformed time-series are then typically analyzed as realizations of a continuous random variable supported on the real line, using established methodologies like state-space methods such as dynamic normal linear models (DLMs: West and Harrison, 1997, Chap. 4) and stochastic volatility (SV: West and Harrison, 1997, Chap. 7) models.

Real-world time series data often exhibit instances where the original values remain unchanged over certain time intervals, resulting in exact zeros in first differences or rates of change (Hautsch et al., 2013; Kömm and Küsters, 2015; Sucarrat and Grønneberg, 2020). In particular, these instances of exact zeros frequently arise in economic datasets; stocks with small market capitalization or low trading volumes often experience periods of price stasis, leading to zero returns during those intervals. Private real estate investment trust (i.e., REIT) indices may exhibit zeros due to unobserved data points that are imputed using the most recent available value: a common practice in applied settings. Conventional state-space models such as DLMs which assume continuous response can be unsuitable in the presence of such zeros, as location estimates may be biased toward zero and variance may be underestimated, which is particularly problematic in applications where accurate estimation of time-varying means or volatilities is critical.

A similar phenomenon is observed in lower-level disaggregated consumer price index (CPI) data, which has motivated this study. Kömm and Küsters (2015) document frequent exact zeros in weekly price changes for skimmed whey powder in Germany, attributing these to censoring and insufficient information. We also illustrate in the subsequent section using monthly CPI data from four countries — the US, UK, Germany, and Japan — that factors such as the mode of data collection practices contribute to price staleness. Macroeconomic literature further highlights time- and state-dependent firm-level price

adjustment behaviors to explain variations in the timing of price changes within firms (Klenow and Kryvtsov, 2008; Nakamura and Steinsson, 2008; Dixon and Grimme, 2022), asserting price adjustment behaviors at a sub-monthly frequency, potentially explaining price staleness.

Despite the occurrence of zero-inflation, prominent nonstationary stochastic volatility models designed for analyzing trend-inflation and their volatility have largely overlooked the phenomenon of price staleness. This is because these models were primarily developed to capture the distinctive characteristics of *aggregate* inflation data, where price staleness is less pronounced. Namely, the seminal unobserved components model with stochastic volatility (UCSV: Stock and Watson, 2007) has become a widely adopted framework for modeling and forecasting aggregate inflation (Faust and Wright, 2013), with several methodological extensions proposed to refine its application to aggregate measures (e.g., Chan, 2013; Chan et al., 2013, 2016; Chan, 2017; Hwu and Kim, 2019; Zhang et al., 2020; Huber and Pfarrhofer, 2021).

While there also exists models which account for zero-inflation and/or disaggregate measures, they are generally designed solely for predictive purposes and lack the capability to estimate trends and volatilities. For example, Kömm and Küsters (2015) used a univariate ARMA-GARCH model with a threshold mechanism for zeros. Barkan et al. (2023) employed hierarchical recurrent neural networks for disaggregated CPI forecasting. Powell et al. (2017) used autoregressive models for forecasting disaggregated CPI based on monthly data and daily web-scraped prices. The ability to estimate trends and volatilities with UCSV-type models are crucial as they are key features of macroeconomic time series data (Primiceri, 2005; Nakajima, 2011), and serve as important information for policymakers and for financial institutions in shaping policy and financing strategies.

Alternative existing Bayesian approach are models for censored time-series data such as (dynamic) Tobit models (Chib, 1992; Wei, 1999; Li and Zheng, 2008; Liu et al., 2023). However, the unidirectional censoring assumption is unsuitable for CPI inflation, which can take both positive and negative values, and more broadly zero-inflated continuous time series over the real line. Latent threshold approaches (Nakajima and West, 2013a,b) may be appropriate if rounding is determined to be the sole cause of price staleness. However, as we demonstrate in the following section, this is not the case. An alternative lies in

dynamic models for zero-inflated data using discrete-valued sampling distributions. Such approaches are commonly found in the financial econometrics literature, where there is interest in modeling zero-inflation in discrete price movements observed in high-frequency financial transaction data ([Hausman et al., 1992](#); [Rydberg and Shephard, 2003](#); [Bien et al., 2011](#)). In our specific case, the challenge requires simultaneously accommodating continuous observations and zero-inflation.

We develop a zero-inflated multivariate stochastic volatility model. We do so by generalizing the (UC)SV model by explicitly specifying the exact-zero generating process alongside the (UC)SV-driven nonzero generating process, as a joint Bayesian model based on the dynamic generalized linear model [DGLM] ([West et al. 1985](#); [West and Harrison 1997](#), Chap. 14). In modeling the exact-zero-generating component, we incorporate the latent dynamic logistic model to allow for heterogeneous cross-sectional propensity, temporal persistence, and cross-correlation in zeros.

The idea of specifying the zero-generating process by using the dynamic logistic model can be seen in cases with discrete zero-inflated observations (e.g. [Berry and West, 2020](#); [Lavine et al., 2022](#)), while our usage is for continuous response with stochastic volatility. A related study by [Yanchenko et al. \(2023\)](#) investigates zero-inflated household expenses combining a dynamic logistic model for zeros and Normal dynamic linear models. While similar, our methodology is for continuous response over the real line, designed to additionally account for non-stationarities in variance.

In posterior computation, where the conditional posterior is intractable due to binomial likelihoods with a logistic link function, we utilize the Pólya-Gamma augmentation to restructure the intractable component as conditionally Gaussian and linear ([Polson et al., 2013](#)). The augmentation enables us to construct a fast and efficient custom Gibbs sampler, where we can sample the state variables jointly ([Windle et al., 2013](#); [Glynn et al., 2019](#)). This contrasts the variational Bayesian approach to DGLMs ([West et al., 1985](#)) designed for online, real-time forecasting for fast yet approximate posterior computation, whereas our MCMC-based approach provides asymptotically exact inference for time-varying trends and volatilities which we have justified is crucial. Now, the presented model and sampler are devised for modeling and forecasting CPI inflation data, but the flexible nature of DGLMs suggests wide applicability of our approach to a variety of real-valued multivariate

time-series involving nonstationary and zero-inflation.

The rest of the paper is structured as follows. Section [2] introduces the disaggregated CPI data and provides background on the occurrence of zeros. Section [3] presents the proposed zero-inflated (UC)SV and M(UC)SV models, along with a brief overview of the posterior sampling algorithm. Section [5] applies the model to highlight the benefits of accounting for zero-inflation and the potential risks of ignoring zero-inflation. Section [5.3] reports the results of a forecasting exercise. Section [6] concludes the paper.

Notation $[T] = \{1, \dots, T\}$ is the set of positive integers upto T . $N(\boldsymbol{\mu}, \boldsymbol{\Sigma})$ represents the Normal distribution with mean and covariance $(\boldsymbol{\mu}, \boldsymbol{\Sigma})$, and $N(\boldsymbol{x} \mid \boldsymbol{\mu}, \boldsymbol{\Sigma})$ is its density evaluated at \boldsymbol{x} . $IG(\alpha, \beta)$ represents the inverted Gamma distribution with density $IG(x \mid \alpha, \beta) \propto x^{-(\alpha+1)} \exp(-\beta/x)$. $BIN(n, p)$ is the Binomial distribution with n trials and success probability p .

2 Disaggregated consumer price indices

2.1 Consumer price index

CPI is calculated hierarchically. Using the Japanese CPI as a specific example, we provide a precise and detailed description of this process, though the basic structure is common across most developed countries.

At the lowest level of the hierarchy, the index at the time-item-location level is calculated by averaging month-item-municipality-store-specific surveyed prices collected from different retail stores. These input prices are obtained through the monthly Trend Survey of the Japanese Retail Price Survey, an official statistical survey. This data is then compiled into a time-item-level index by taking a weighted average over municipalities.

Subsequently, a higher-level index, referred to as the minor groups index, is computed by averaging across items using weights. This process continues sequentially to calculate progressively higher-level indices, resulting in the following hierarchy: the item-level, minor groups, subgroups (item-category level), 10 major groups (sectoral level), and finally, the aggregate index.

Table [1] illustrates this hierarchy by listing ten representative items selected from each of the 10 major groups. The breakdown demonstrates a highly granular structure.

<i>All items</i>	<i>10 Major (Sectoral)</i>	<i>Sub (Item-category)</i>	<i>Items</i>
All	Fuel, light & water charges	Electricity	Electricity
	Medical care	Medical services	Medical treatment
	Transport. & comm.	Communication	Letters
	Education	Tutorial fees	Elementary school
	Food	Fruits	Apples
	Clothes & footwear	Footwear	Men’s shoes
	Housing	Rent	House rent, private
	Furniture & household utens.	Durable goods	Microwave ovens
	Culture & recreation	Durable goods	TV sets
	Miscellaneous	Personal effects	Suitcases
Count	10	49	582

Table 1: A tabulated example of ten items recorded in CPI. **Note 1:** the table takes the Japanese CPI as an example to provide a precise and detailed example. The hierarchical structure is applicable to most other developed countries. **Note 2:** for a full list of component names for all four countries, see the appendix.

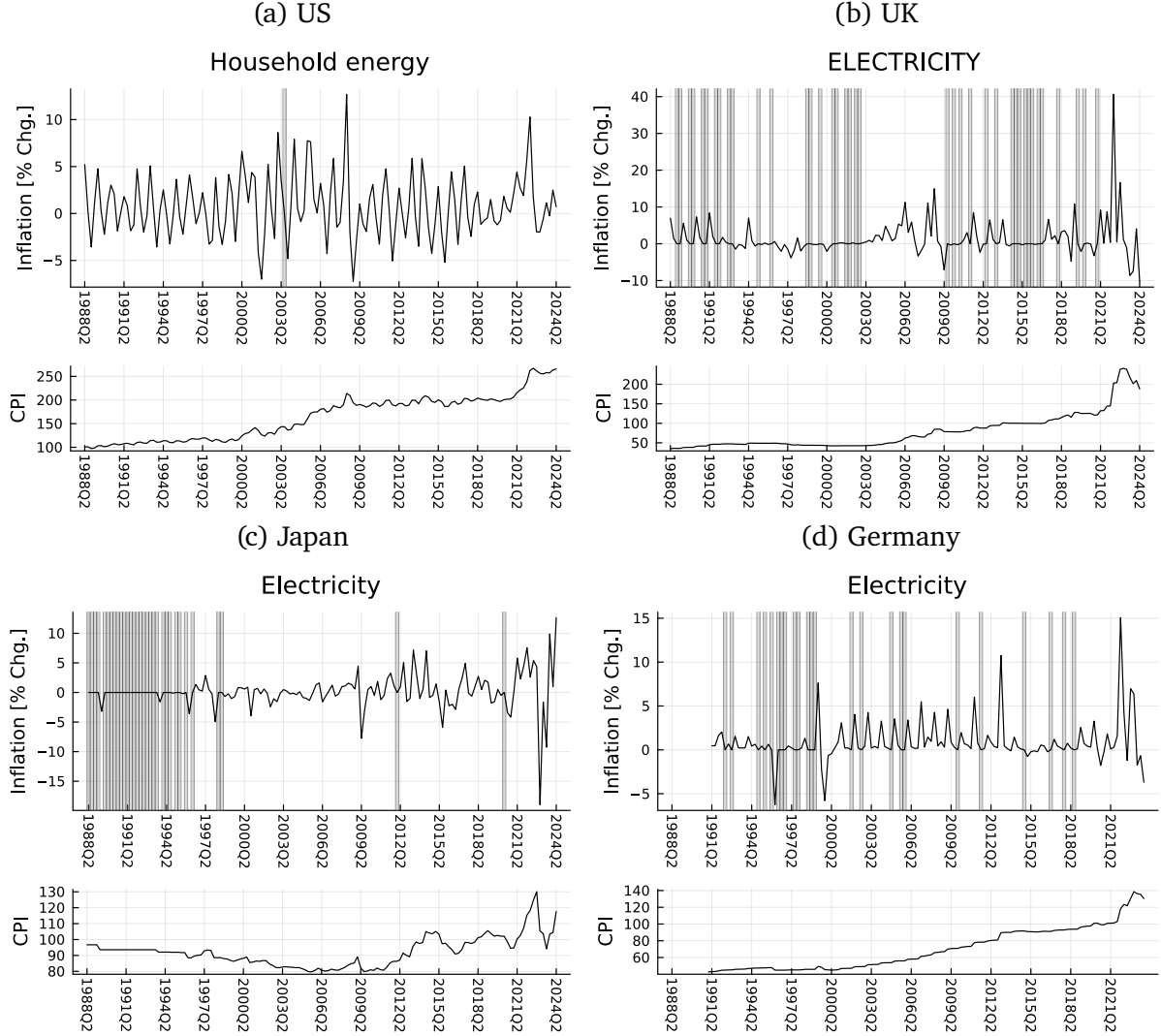
2.2 Measurement error due to data collection

Figure [1] visualizes one of the disaggregated components for the US, UK, Germany, and Japan. Notably, zeros are prevalent in some of the indices. We discuss various relevant perspectives on this phenomenon and outline the desirable characteristics of our proposed model.

A key reason for the occurrence of zeros is the combination of (1) infrequent within-firm price adjustments, (2) the mode of data collection, and (3) rounding. For each item-level index, the respective principal statistical agency of a given country typically pre-determines a set of representative products — often a singleton set — subject to repeated price data collection. The data collection process is also meticulously designed to capture price fluctuations in a cost-efficient manner, specifying details such as the store, brand, quantity/size, unit of sales, area of production, and model number.

This implies that the observed price staleness reflects that of the specific item of a particular firm at a specific time and location, rather than the overall behavior of the representative item. Additionally, some statistical agencies (e.g., the BLS in the US and the

Figure 1: Time-series plot of the electricity component for four selected countries. The comparison highlights four key characteristics of the data: (1) occurrences of exact zeros, (2) heterogeneity in the frequency and persistence of zeros, (3) non-stationarity in the non-zero component, and (4) inevitable missing values prior to component-level data collection. Note: Gray shaded regions indicate periods of observed price staleness.



SBJ in Japan) acknowledge that month-item-municipality-specific indices may be missing, such as when an item is discontinued in the surveyed municipality. In such cases, the item and its weight may be excluded from the calculation of higher-level indices, representing another instance of information scarcity.

Combined with the fact that not all firms adjust prices on a monthly or even quarterly basis (Higo and Saita, 2007; Dixon and Grimme, 2022), the inevitable scarcity of information can result in apparent price staleness. Therefore, the model should incorporate an additional layer of uncertainty to account for the discrepancy between the observed data and the underlying price dynamics we aim to measure.

Figure [2] provides a comprehensive view of the sparsity patterns in the data. It reveals substantial variation in the proportions of sparsity, with the proportion of exact zeros ranging from single-digit percentages to instances where non-zero observations are rare. Cross-sectional heterogeneity in zero inflation is a fundamental characteristic of the data that the model must capture.

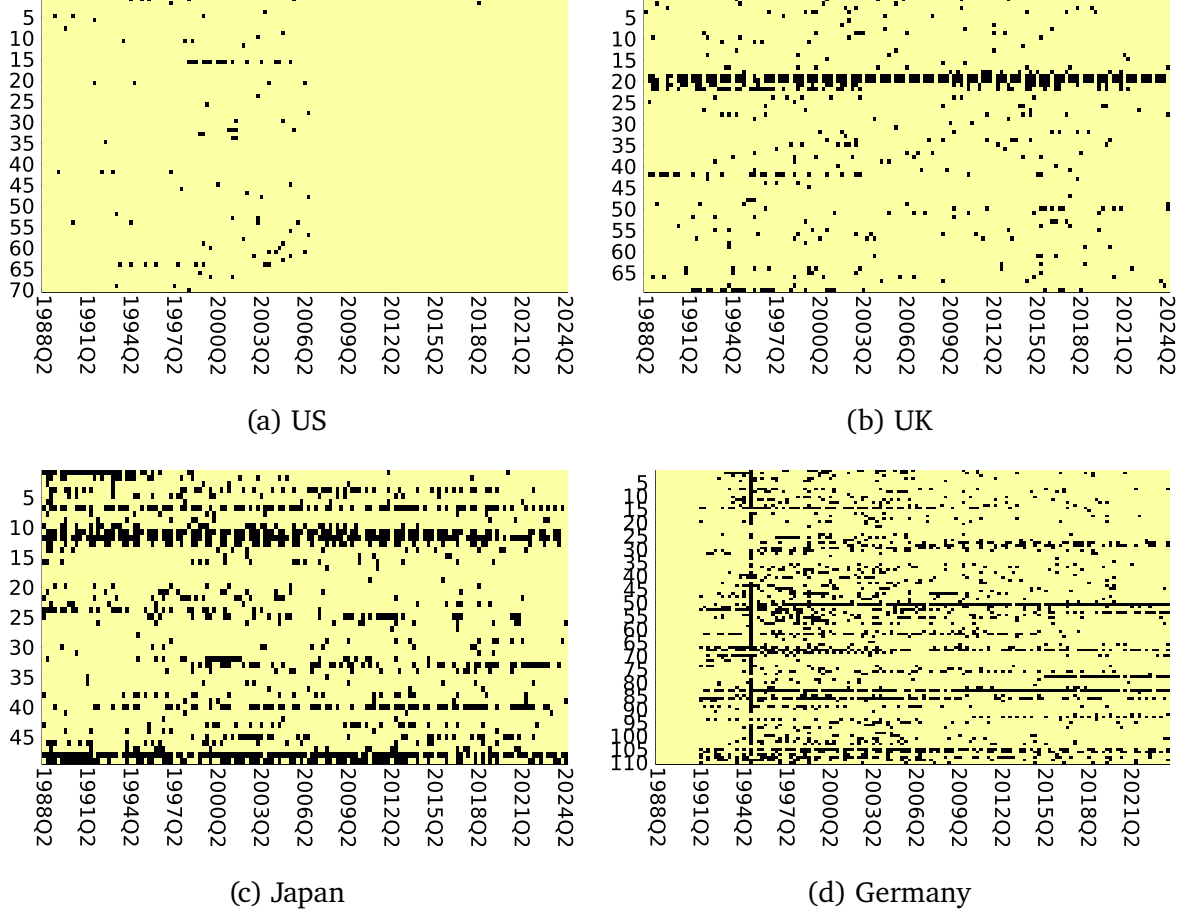


Figure 2: Heatmap of the sparsity patterns in the inflation time series. **Note:** Black represents zeros, while yellow represents non-zeros. Zeros in the US CPI data significantly decreased after 2007 due to an improvement in decimal precision, where values were truncated to three decimal places instead of one.

2.3 Intra- and inter-component dependence

We also observe inter-temporal persistence in zero-inflation, which arises due to various factors. One such factor is systematic institutional restrictions. Figure [1c] illustrates this with quarterly inflation for Japanese electricity bills. Prior to the 1995 revision of the Electricity Business Act (1995:Q4), which initiated energy liberalization in Japan, elec-

tricity prices were significantly stale, with persistent zeros. Such items are subject to price revisions only after administrative processes, leading to observable inflation occurring intermittently and contributing to the persistence of zeros.

Other items, such as medical services or school fees, similarly exhibit high proportions of zeros. Conversely, items whose prices are largely market-driven, such as fuel or food, are less prone to zero inflation. Capturing within-component inter-temporal persistence of zeros (or its absence) is thus a key requirement for the model.

2.4 Missing values and non-stationarity

Missing values are a common issue in disaggregated CPI data, as illustrated in Figure [3] with two examples. This arises because the starting date of data collection varies by item. Additionally, for some items, the frequency of data collection deviates from the standard monthly schedule.

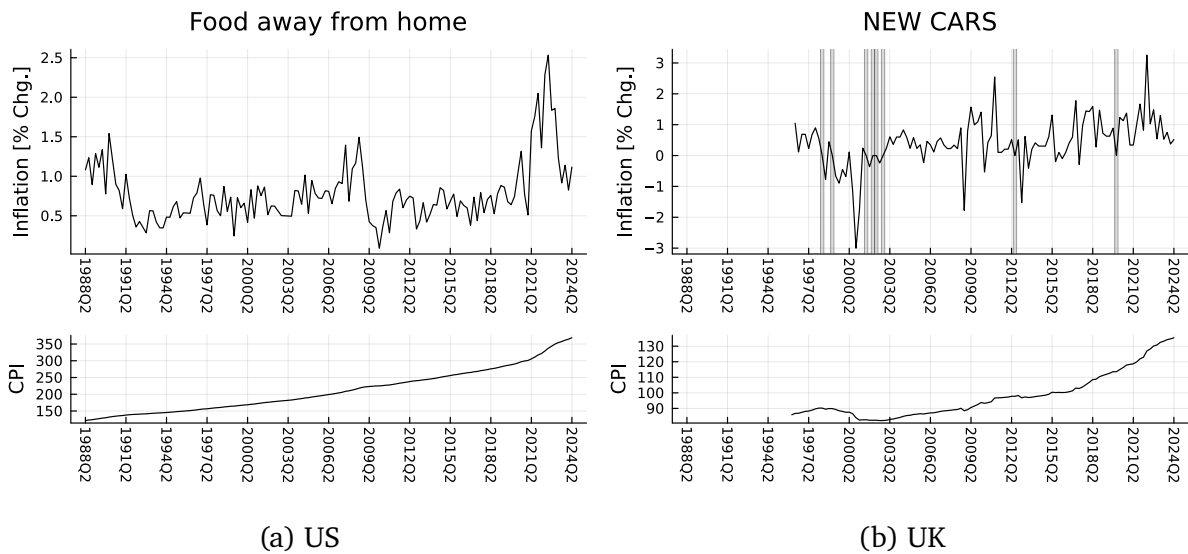


Figure 3: Time-series plot of the *food away from home* component in the US and *new cars* in the UK. **Note:** Gray shaded regions indicate observed price staleness.

The nonzero component, on the other hand, exhibits substantial non-stationarities, as shown in Figure [3]. Moreover, while we know that inter-component dependencies exist in the non-stationarity patterns (e.g., items within the same major category often exhibit comovements, and non-core components such as electricity or gasoline tend to influence most other components), these comovements cannot be reliably estimated from simple summary statistics due to the prevalence of missing data; see Figure [4].

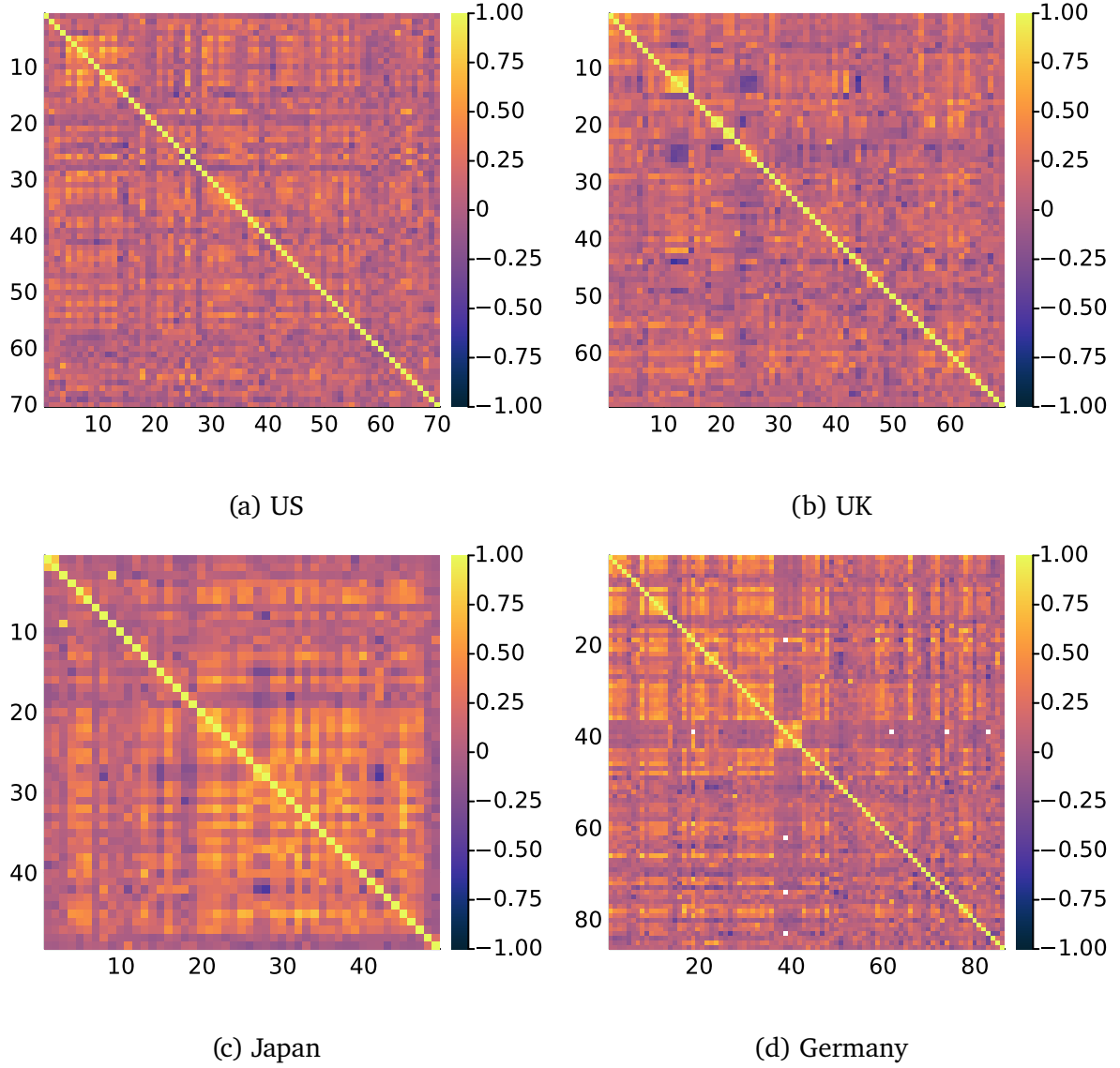


Figure 4: Heatmap of the empirical correlation matrix of the observations, including both zero and nonzero observations. **Note 1:** blank white entries are missing values due to no overlap. **Note 2:** for a full list of component names, see the appendix.

2.5 Summary

We summarize the desirable features of the zero-inflated model as follows. Following [Berry and West \(2020\)](#), it is desirable to model both the zero and nonzero data within a joint probabilistic framework. For the zero component, the model should capture heterogeneity in the propensity of zeros, temporal persistence, and potential cross-series dependencies in the zero-generating mechanism. For the nonzero component, the model should account for possible comovements across the cross-sectional dimension of the multivariate time series. The empirical pairwise correlations visualized in Figure [3] support this view.

Additionally, the model should retain the ability to estimate trends and stochastic volatilities, consistent with established models in the literature (e.g., [Stock and Watson, 2007, 2016](#); [Eo et al., 2023](#)).

In the following section, we present a multivariate stochastic volatility model with zero inflation that addresses these requirements.

3 The model

3.1 Time-varying probability of zero

We first propose a univariate formulation of the univariate zero-inflated UCSV (Z-UCSV) model. Let $y_{1:T} := (y_1, \dots, y_T)^\top \in \mathbb{R}^T$ represent the univariate observations. Let $\theta_{1:T} := (\theta_1, \dots, \theta_T)^\top$ and $h_{1:T} := (h_1, \dots, h_T)^\top$ be the unobserved trend and measurement log-volatility.

The UCSV model we consider relates the triple $(y_{1:T}, \theta_{1:T}, h_{1:T})$ by

$$y_t = \theta_t + \varepsilon_t^{(y)}, \quad \varepsilon_t^{(y)} | h_t \stackrel{ind}{\sim} N_1(0, \exp h_t) \quad (1)$$

$$\theta_t = \theta_{t-1} + \varepsilon_t^{(\theta)}, \quad \varepsilon_t^{(\theta)} | g_t \stackrel{ind}{\sim} N_1(0, \sigma_\theta^2), \quad (2)$$

$$h_t = h_{t-1} + \varepsilon_t^{(h)}, \quad \varepsilon_t^{(h)} | \sigma_h^2 \stackrel{ind}{\sim} N_1(0, \sigma_h^2) \quad (3)$$

where $N_D(\boldsymbol{\mu}, \boldsymbol{\Sigma})$ is used to denote the D -dimensional Normal distribution with mean and covariance $(\boldsymbol{\mu}, \boldsymbol{\Sigma})$. The index runs through $t \in [T] := \{1, \dots, T\}$. The variances terms $\sigma_g^2, \sigma_h^2 \in \mathbb{R}_{>0}$ and the initial states $\theta_0, g_0, h_0 \in \mathbb{R}$ are also random variables to be particularized later with priors.

The time-varying conditional means, $\theta_{1:T}$, are often referred to as a latent trend component or trend inflation ([Stock and Watson, 2007](#); [Chan, 2013](#); [Chan et al., 2013, 2016](#); [Stock and Watson, 2016](#); [Li and Koopman, 2021](#); [Eo et al., 2023](#)), reflecting the belief that the underlying process governing the permanent level of inflation evolves smoothly and is unobservable. Movements in the trend are typically seen as permanent and potentially persistent shifts in the inflation level. In contrast, the deviation from this trend, $y_{1:T} - \theta_{1:T}$, is interpreted as a transient and temporary stochastic shock around the permanent level, also known as the inflation gap ([Cogley et al., 2010](#); [Hwu and Kim, 2019](#)).

The log-volatility process in the measurement equation, $h_{1:T}$, is often regarded as transitory volatility. The original formulation also includes a second log-volatility process in the transition equation, representing permanent volatility. However, this component is omitted in our model, given that variations in volatility are much less pronounced at the item-specific level. Similar modeling assumptions are also implemented in existing literature (e.g., [Chan, 2013](#)).

From here, we introduce three additional and key latent stochastic processes: $y_{1:T}^* := (y_1^*, \dots, y_T^*)^\top \in \mathbb{R}^T$, $p_{1:T} := (p_1, \dots, p_T)^\top \in (0, 1)^T$ and $\pi_{1:T} := (\pi_1, \dots, \pi_T)^\top \in \mathbb{R}^T$. We specify a latent dynamic logistic model, a special case of DGLM ([West et al. 1985](#); [West and Harrison 1997](#), Chap. 14) by

$$y_t | y_t^*, p_t \stackrel{\text{ind}}{\sim} (1 - p_t)\delta_{y_t^*} + p_t\delta_0, \quad (4)$$

$$y_t^* = \theta_t + \varepsilon_t^{(y)}, \quad (5)$$

$$p_t = \text{logit}^{-1}(\pi_t), \quad (6)$$

$$\pi_t = \pi_{t-1} + \varepsilon_t^{(\pi)}, \quad \varepsilon_t^{(\pi)} | \sigma_\pi^2 \stackrel{\text{ind}}{\sim} \text{N}_1(0, \sigma_\pi^2). \quad (7)$$

The triple $(\theta_{1:T}, h_{1:T})$ inherits the same dynamical specification in eq. (2), (3), but not eq. (1). δ_c is the point-mass distribution with the mass at $c \in \mathbb{R}$. In eq. (4), note that $y_{1:T}$ need not equate to the almost-surely non-zero $y_{1:T}^*$ *a priori*; this reflects the discrepancy between what we observe and what we want to measure, described in sec. [2]. The autonomous probabilities $p_{1:T}$ are granted persistence via a Markovian structure $p(\pi_{1:T} | \sigma_\pi^2, \pi_0) = \prod_{t=1}^T p(\pi_t | \pi_{t-1}, \sigma_\pi^2)$.

The model is completed with priors on the static parameters and initial states:

$$\sigma_\theta^2 \sim \text{IG}(\alpha_\theta, \beta_\theta), \quad \sigma_h^2 \sim \text{IG}(\alpha_h, \beta_h), \quad \sigma_\pi^2 \sim \text{IG}(\alpha_\pi, \beta_\pi), \quad (8)$$

$$\theta_0 \sim \text{N}_1(\mu_{\theta_0}, \sigma_{\theta_0}^2), \quad h_0 \sim \text{N}_1(\mu_{h_0}, \sigma_{h_0}^2), \quad \pi_0 \sim \text{N}_1(\mu_{\pi_0}, \sigma_{\pi_0}^2). \quad (9)$$

In summary, the observed univariate time-series $y_{1:T}$ relates to the unobserved collection of interest,

$$\Theta := (y_{1:T}^*, \theta_{0:T}, h_{0:T}, \pi_{0:T}, \sigma_\theta^2, \sigma_h^2, \sigma_\pi^2), \quad (10)$$

via the joint distribution with prior hyper-parameters $(\mu_{\theta_0}, \mu_{\pi_0}, \mu_{h_0}, \sigma_{\pi_0}^2, \sigma_{\theta_0}^2, \sigma_{h_0}^2)$:

$$p(y_{1:T}, \Theta) = p(\theta_0)p(h_0)p(\sigma_{\theta}^2)p(\pi_0)p(\sigma_h^2)p(\sigma_{\pi}^2) \\ \times \prod_{t=1}^T p(\theta_t|\theta_{t-1}, \sigma_{\theta}^2)p(h_t|h_{t-1}, \sigma_h^2)p(y_t^*|\theta_t, h_t)p(\pi_t|\pi_{t-1}, \sigma_{\pi}^2)\mathbb{P}(y_t|y_t^*, \pi_t).$$

The Z-UCSV model contains the UCSV model of [Stock and Watson \(2007\)](#) as a special case *a priori* under some conditions. If we let $\pi_t \rightarrow -\infty$ for $t \in [T]$, then it must hold in the limiting model $p_t = 0$ for $t \in [T]$, in which case

$$y_t = y_t^* = \theta_t + \varepsilon_t^{(y)}. \quad (11)$$

3.2 Posterior inference

We provide an overview of a custom Gibbs sampler to perform posterior inference. A detailed exposition is provided in the appendix. Gibbs sampling is performed in blocks as follows.

- (1) Sample the initial states (θ_0, h_0, π_0) given $(\theta_1, h_1, \pi_1, \sigma_{\theta}^2, \sigma_h^2, \sigma_{\pi}^2)$.
- (2) Sample the static parameters $(\sigma_{\theta}^2, \sigma_h^2, \sigma_{\pi}^2)$ given $(\theta_{0:T}, h_{0:T}, \pi_{0:T})$.
- (3) Sample the latent trend $\theta_{1:T}$ given $(\theta_0, \sigma_{\theta}^2, y_{1:T}^*)$.
- (4) Sample the stochastic volatility $h_{1:T}$ given $(h_0, \sigma_h^2, \theta_{1:T}, y_{1:T}^*)$.
- (5) Sample the dynamic probabilities $p_{1:T}$ given $(\pi_0, \sigma_{\pi}^2, y_{1:T})$.
- (6) Data-augment nonzero $y_{1:T}^*$ given $(\theta_{1:T}, h_{1:T}, y_{1:T})$.

In steps (1) and (2), the static parameters and initial states may be readily simulated from Normals or inverted Gammas. In step (3), the full conditional posterior of the latent trend is dynamic, linear, and Normal; sampling is doable using any usual apparatus to sample the latent states in a linear and Normal state-space model. We make use of the forward-filtering backward-sampling (FFBS) algorithm ([Carter and Kohn, 1994](#); [Frühwirth-Schnatter, 1994](#)). In step (4), the log-volatility processes is efficiently samplable via auxiliary Normal mixtures ([Kim et al., 1998](#)). We make use of the ten-component mixture approximation ([Omori et al., 2007](#)). The states are then sampled

jointly using precision samplers (Chan and Jeliazkov, 2009) for its efficiency. In step (6), the posterior is augmented with nonzero data sampled from Normals.

Step (5) encompasses sampling from the full conditional posterior of the dynamic pre-transformed probabilities $p(\pi_{1:T} \mid \pi_0, \sigma_\pi^2, y_{1:T})$ that involves logistic transformations and Binomial likelihoods. To do so efficiently, first introduce auxiliary sparsity indicators $\gamma_{1:T} := (\gamma_1, \dots, \gamma_T)^\top$ where $\gamma_t \mid p_t \stackrel{\text{ind}}{\sim} \text{BIN}(1, p_t)$, and replace the measurement equation in eq. (4) with $y_t = y_t^* \mathbb{I}\{\gamma_t = 0\}$, where $\mathbb{I}\{\cdot\}$ is an indicator function. The *likelihoods* on $\gamma_{1:T}$ are also re-written via augmented likelihoods $p(\gamma_t, \omega_t \mid \pi_t)$ over $t \in [T]$:

$$\begin{aligned} \mathbb{P}(\gamma_t \mid \pi_t) &= \frac{(\exp \pi_t)^{\gamma_t}}{1 + \exp \pi_t} = \int_0^\infty p(\gamma_t, \omega_t \mid \pi_t) d\omega_t \\ &= \int_0^\infty 2^{-1} \exp\{(\gamma_t - 1/2)\pi_t\} \exp\{-\omega_t \pi_t^2/2\} \text{PG}(\omega_t \mid 1, 0) d\omega_t. \end{aligned}$$

$\text{PG}(\cdot \mid 1, 0)$ is the probability density of the Pólya-Gamma distribution $\text{PG}(1, 0)$ following the conventional notation (Polson et al., 2013; Windle et al., 2013). With a prior density $p(\pi_{1:T} \mid \pi_0, \sigma_\pi^2)$, the joint distribution is locally re-expressed by

$$\begin{aligned} p(\pi_{1:T}, \gamma_{1:T} \mid \pi_0, \sigma_\pi^2) &= p(\pi_{1:T} \mid \pi_0, \sigma_\pi^2) \prod_{t=1}^T \int_0^\infty p(\gamma_t, \omega_t \mid \pi_t) d\omega_t \\ &= \int_{\mathbb{R}_{>0}^T} p(\pi_{1:T} \mid \pi_0, \sigma_\pi^2) p(\gamma_{1:T}, \omega_{1:T} \mid \pi_{1:T}) d\omega_{1:T}, \end{aligned}$$

where $\omega_{1:T} := (\omega_1, \dots, \omega_T)^\top$. The integrand in the above characterizes a conditional joint distribution on $(\pi_{1:T}, \gamma_{1:T}, \omega_{1:T})$ that admits $p(\pi_{1:T}, \gamma_{1:T} \mid \pi_0, \sigma_\pi^2)$ as its marginal, and facilitates efficient sampling from the target $p(\pi_{1:T} \mid \pi_0, \sigma_\pi^2, \gamma_{1:T}) \propto p(\pi_{1:T}, \gamma_{1:T} \mid \pi_0, \sigma_\pi^2)$ via conditioning on $\omega_{1:T}$, performed in two steps. First, given $\pi_{1:T}$, sample from

$$p(\omega_{1:T} \mid \pi_{1:T}) \propto \prod_{t=1}^T \text{PG}(\omega_t \mid 1, \pi_t).$$

Next, given $\omega_{1:T}$, sample from

$$p(\pi_{1:T} \mid \pi_0, \sigma_\pi^2, \gamma_{1:T}, \omega_{1:T}) \propto \underbrace{p(\pi_{1:T} \mid \pi_0, \sigma_\pi^2)}_{\text{Linear Normal Latent State}} \underbrace{\prod_{t=1}^T \exp\left\{-\frac{\omega_t}{2} \left(\frac{\kappa_t}{\omega_t} - \pi_t\right)^2\right\}}_{\text{Independent Normal "Likelihood"}},$$

where $\kappa_t := \gamma_t - 1/2$ for $t \in [T]$. Since the *prior* was specified to be a conditionally linear and Normal in eq. (7), we may simply rely on, say the FFBS algorithm.

We remind that other sampling strategies are applicable, but upon reparameterisations or permitting more layers of augmentation (Albert and Chib, 1993; Held and Holmes,

2006; Frühwirth-Schnatter and Frühwirth, 2007). Generic gradient-based Markov-chain Monte Carlo (MCMC) algorithms such as Hamiltonian Monte Carlo (HMC) (Neal, 2011) are also applicable to sample the dynamic probabilities, using a HMC-within-Gibbs scheme. A reason to employ Pólya-Gamma augmentation over other schemes is that the augmentation is least computationally prohibitive. Although the efficiency gains may be inconsequential, for instance, on the original univariate UCSV model, they become increasingly appealing as the dimension of the time-series becomes greater, such as in our application.

3.3 Digression: semi-continuous DLM with custom discrete meshes

Inflation over discrete meshes, not necessarily restricted to zero, can be modeled by modifying the measurement equation to include a point mass that assigns positive probability to a finite set of discrete meshes. This is however a digression; the models that appear in this paper concerns zero-inflation.

The extension is achieved straightforwardly by modifying the measurement equation

$$y_t \sim \sum_{s \in \mathcal{S}} p_{t,s} \delta_s + \left(1 - \sum_{s \in \mathcal{S}} p_{t,s}\right) \mathcal{N}(\mu_t^{(y)}, v_t^{(y)}),$$

where $(\mu_t^{(y)}, v_t^{(y)})$ specifies the time-varying location and scale. An example where such modifications are relevant is one-inflated data which commonly arise in psychometric item response theory models (see Müller, 1987; Ospina and Ferrari, 2012; Noel and Dauvier, 2007) of continuous-bounded proportions (where it may be also sensible to relax the Normality assumption as needed). The issue of systematic discrete meshes on an unbounded support is relevant in accounting research, where phenomena like rounding of reported earnings are prevalent (Thomas, 1989; Das and Zhang, 2003). The dynamic logistic sub-model shall then be extended to a dynamic multinomial logistic sub-model, where probabilities are jointly assigned to individual points on the discrete meshes at each time step. Posterior inference is similarly feasible via Gibbs sampling algorithm leveraging the Pólya-Gamma augmented FFBS. Specifics are provided in the appendix.

4 Multivariate extension

We now consider a multivariate extension with cross-sectional dependence structure. We redefine notations by introducing a new index $k \in [K]$ that indexes the k -th time-series, where K is fixed. Let $y_{t,k} \in \mathbb{R}$ represent the k -th observable time-series at time $t \in [T]$, and $\mathbf{y}_t := (y_{t,1}, \dots, y_{t,K})^\top \in \mathbb{R}^K$. Similarly allocate the k -th latent trend, state log-volatility, and measurement log-volatility indexed at time $t \in [T]$ to $\theta_{t,k}, h_{t,k} \in \mathbb{R}$, and compile these as $\boldsymbol{\theta}_t := (\theta_{t,1}, \dots, \theta_{t,K})^\top, \mathbf{h}_t := (h_{t,1}, \dots, h_{t,K})^\top \in \mathbb{R}^K$. In addition, let $p_{t,k} := \mathbb{P}(y_{t,k} = 0 \mid \pi_{t,k}) \in (0, 1)$, parameterized by $\pi_{t,k} \in \mathbb{R}$. We write $\mathbf{y}_{1:t'}$ to query the first $t' \in [T]$ observations.

We specify the multivariate zero-inflated UCSV [Z-MUCSV] model as follows.

$$\begin{aligned}
y_{t,k} \mid p_{t,k}, y_{t,k}^* &\stackrel{\text{ind}}{\sim} (1 - p_{t,k})\delta_{y_{t,k}^*} + p_{t,k}\delta_0, & (k \in [K]) \\
\mathbf{y}_t^* \mid \boldsymbol{\theta}_t, \boldsymbol{\Sigma}_t^{(y)}, \mathbf{h}_t &\stackrel{\text{ind}}{\sim} \mathbf{N}_K(\boldsymbol{\theta}_t, \boldsymbol{\Sigma}_t^{(y)}(\mathbf{h}_t)), \\
\boldsymbol{\theta}_t \mid \boldsymbol{\theta}_{t-1}, \sigma_{(\theta),1}^2, \dots, \sigma_{(\theta),K}^2 &\stackrel{\text{ind}}{\sim} \mathbf{N}_K(\boldsymbol{\theta}_{t-1}, \text{diag}(\sigma_{(\theta),1}^2, \dots, \sigma_{(\theta),K}^2)), \\
\mathbf{h}_t \mid \mathbf{h}_{t-1}, \sigma_{(h),1}^2, \dots, \sigma_{(h),K}^2 &\stackrel{\text{ind}}{\sim} \mathbf{N}_K(\mathbf{h}_{t-1}, \text{diag}(\sigma_{(h),1}^2, \dots, \sigma_{(h),K}^2)), \\
p_{t,k} &= \text{logit}^{-1}(\pi_{t,k}), & (k \in [K]) \\
\boldsymbol{\pi}_t \mid \boldsymbol{\pi}_{t-1}, \boldsymbol{\Sigma}^{(\pi)} &\stackrel{\text{ind}}{\sim} \mathbf{N}_K(\boldsymbol{\pi}_{t-1}, \boldsymbol{\Sigma}^{(\pi)}).
\end{aligned}$$

We specify priors over $k \in [K]$ by $\theta_{0,k} \stackrel{\text{ind}}{\sim} \mathbf{N}_1(\mu_{\theta_{0,k}}, \sigma_{\theta_{0,k}}^2)$, $h_{0,k} \stackrel{\text{ind}}{\sim} \mathbf{N}_1(\mu_{h_{0,k}}, \sigma_{h_{0,k}}^2)$, $\pi_{0,k} \stackrel{\text{ind}}{\sim} \mathbf{N}_1(\mu_{\pi_{0,k}}, \sigma_{\pi_{0,k}}^2)$, $\sigma_{(\theta),k}^2 \stackrel{\text{ind}}{\sim} \text{IG}(\alpha_{(\theta),k}, \beta_{(\theta),k})$, and $\sigma_{(h),k}^2 \stackrel{\text{ind}}{\sim} \text{IG}(\alpha_{(h),k}, \beta_{(h),k})$. Analogous to the univariate case, \mathbf{y}_t^* , is not necessarily assumed to be observed; the equality $y_{t,k} = y_{t,k}^*$ need not necessarily hold.

4.1 Order-invariant inter-component dependence

If the covariance matrices, $\boldsymbol{\Sigma}_t^{(y)}$ and $\boldsymbol{\Sigma}^{(\pi)}$, are diagonal, then the multivariate model reduces to K Z-UCSV models with no inter-component dependence. This is false as described in section [2]. To introduce and infer such dependencies, we let $\boldsymbol{\Sigma}^{(\pi)} \sim \text{IW}(\nu_\pi, \mathbf{S}_\pi)$, where $\text{IW}(\nu, \mathbf{S})$ is an inverse Wishart distribution with degrees of freedom $\nu > K - 1$ and \mathbf{S} a $K \times K$ positive definite scale matrix.

A common approach to specifying inter-component dependence while preserving the time-varying volatility structure is through the Cholesky SV parameterization.

$$\boldsymbol{\Sigma}_t^{(y)}(\mathbf{h}_t) = \mathbf{C}^{-1} \text{diag}(\exp h_{t,1}, \dots, \exp h_{t,K}) \mathbf{C}^{-\top},$$

where $\mathbf{C}^{-1} = [c_{i,j}]_{i,j \in [K]}$ is a strictly lower-triangular matrix of size $(K \times K)$ (Primiceri, 2005; Eo et al., 2023). The strictly lower-triangular entries of the Cholesky factors are unrestricted and follow $c_{i,j} \stackrel{ind}{\sim} \text{N}_1(\mu_{c_{i,j}}, \sigma_{c_{i,j}}^2)$ for $1 \leq j < i \leq K$. This parameterization parsimoniously induces a Normal regression-type relationship among the components, thereby capturing inter-component dependencies while preserving the time-varying volatility structure. Furthermore, it facilitates tractable posterior sampling schemes. However, it is important to note that this parameterization is sensitive to the ordering of the variables; the variation in the trend evolution of the k -th series, $\mathbf{y}_{1:T,k}$, is partially explained by the variations in the preceding series, $\mathbf{y}_{1:T,1:k-1}$.

The choice of variable ordering is critical in our setup, where the number of components ranges from a maximum of 86 (Germany) to a minimum of 49 (Japan). However, assessing the sensitivity of posterior estimates to different orderings is computationally intractable due to the combinatorial explosion of possible permutations. To address this, we adopt an order-invariant parameterization of stochastic volatility (Chan et al., 2024), allowing the matrix \mathbf{C} to remain non-singular but otherwise unrestricted; writing the k -th row of \mathbf{C} as $\mathbf{C}_{k,:}$, let

$$\mathbf{C}_{k,:} \stackrel{ind}{\sim} \text{N}(\mathbf{m}_k^{(C)}, \mathbf{V}_k^{(C)}).$$

Note now that \mathbf{C} is dense and not lower-triangular. Alternative approaches to addressing the dependence on ordering include Levy and Lopes (2024) (and relatedly Frühwirth-Schnatter et al., 2024) who performs posterior inference also upon the series ordering. While this method is applicable, the approach of Chan et al. (2024) suffices for our purposes, as our primary objective is not to infer ordering but to identify time-varying trends, volatilities, and probabilities of zeros in an order-invariant manner.

4.2 Posterior inference

The collection of unobserved parameters of interest in the multivariate case is

$$\Theta := (\theta_{0,1:K}, h_{0,1:K}, \pi_{0,1:K}, \mathbf{h}_{1:T}, \mathbf{C}, \sigma_{(\theta),1:K}^2, \sigma_{(h),1:K}^2, \Sigma^{(\pi)}, \boldsymbol{\theta}_{1:T}, \mathbf{y}_{1:T}^*).$$

The joint distribution of the Z-MUCSV model is

$$p(\Sigma^{(\pi)}) \left(\prod_{k=1}^K p(\mathbf{C}_{k,:}) p(\sigma_{(\theta),k}^2) p(\sigma_{(h),k}^2) p(\theta_{0,k}) p(h_{0,k}) p(\pi_{0,k}) \right) \\ \prod_{t=1}^T p(\boldsymbol{\theta}_t | \boldsymbol{\theta}_{t-1}, \sigma_{(\theta),1:K}^2, \mathbf{L}) p(\boldsymbol{\pi}_t | \boldsymbol{\pi}_{t-1}, \Sigma^{(\pi)}) p(\mathbf{h}_t | \mathbf{h}_{t-1}, \sigma_{(h),1:K}^2) p(\mathbf{y}_t^* | \boldsymbol{\theta}_t, \mathbf{h}_t, \mathbf{C}) \mathbb{P}(\mathbf{y}_t | \mathbf{y}_t^*, \boldsymbol{\pi}_t).$$

Gibbs sampling on the Z-MUCSV model is performed in blocks as follows. A detailed exposition for Z-MUCSV is also provided in the appendix.

- (1) Sample the initial states $(\boldsymbol{\theta}_0, \mathbf{h}_0, \boldsymbol{\pi}_0)$ given $(\boldsymbol{\theta}_1, \mathbf{h}_1, \boldsymbol{\pi}_1, \sigma_{(\theta),1:K}^2, \sigma_{(h),1:K}^2, \Sigma^{(\pi)})$.
- (2) Sample the static parameters $(\sigma_{(\theta),1:K}^2, \sigma_{(h),1:K}^2, \Sigma^{(\pi)})$ given $(\boldsymbol{\theta}_{0:T}, \mathbf{h}_{0:T}, \boldsymbol{\pi}_{0:T})$.
- (3) Sample the latent trend $\boldsymbol{\theta}_{1:T}$ given $(\boldsymbol{\theta}_0, \sigma_{(\theta),1:K}^2, \mathbf{C}, \mathbf{y}_{1:T}^*)$,
- (4) Sample the stochastic volatility $\mathbf{h}_{1:T}$ given $(\mathbf{h}_0, \sigma_{(h),1:K}^2, \mathbf{C}, \boldsymbol{\theta}_{0:T}, \mathbf{y}_{1:T}^*)$.
- (5) Sample the dynamic probabilities $\mathbf{p}_{1:T}$ given $(\boldsymbol{\pi}_0, \Sigma^{(\pi)}, \mathbf{y}_{1:T})$.
- (6) Sample the nonzero data $\mathbf{y}_{1:T}^*$ given $(\boldsymbol{\theta}_{1:T}, \mathbf{h}_{1:T}, \mathbf{C}, \mathbf{y}_{1:T})$.
- (7) Sample \mathbf{C} given $(\mathbf{y}_{1:T}^*, \boldsymbol{\theta}_{0:T}, \mathbf{h}_{1:T})$.

5 Results

5.1 Setup

We now analyze price inflations for the US, UK, Germany, and Japan using item-category-level disaggregated quarterly CPI time-series data with the proposed Z-MUCSV model. For comparison, we also estimate the non-zero-inflated counterpart and evaluate their forecast performance. In all settings, we uniformly align the data’s time span, covering the period from 1988:Q2 to the latest available for all countries.

In both the in- and out-of-sample settings, the prior hyperparameters are set as $(\mu_{\theta_{0,k}}, \sigma_{\theta_{0,k}}^2) = (0, 10)$, $(\mu_{x_{0,k}}, \sigma_{x_{0,k}}^2) = (0, 1)$ for $x \in \{h, \pi\}$, $(\alpha_{(x),k}, \beta_{(x),k}) = (11, 1)$ for $x \in \{\theta, \pi\}$, and $(\alpha_{(h),k}, \beta_{(h),k}) = (101, 1)$. Z-MUCSV is additionally granted $(\nu_\pi, \mathbf{S}_\pi) = (2K, \mathbf{I}_K)$, $\mathbf{m}_k^{(C)} = \mathbf{0}_K$, and $\mathbf{V}_k^{(C)} = K^{-3.5}$. We simulate $R = 10000 + 2000$ MCMC samples and discard the initial 2000 samples. The thinning factor is 20. Data is scaled such that each component has equal standard deviations to facilitate stable posterior computation.

5.2 Full in-sample estimation

5.2.1 Probability of zeros

We begin by presenting the posterior estimates of the probability of zeros in Figure [5]. A key distinction between MUCSV and Z-MUCSV is that the latter assigns non-zero time- and component-specific probabilities of zeros, effectively capturing the zero-inflation dynamics. For instance, Z-UCSVs successfully quantify the significant heterogeneity in price staleness during the periods before and after December 1995 (1995:Q4), showing a rapidly declining time-specific probability of zeros. This period corresponds to the 1995 revision of the Electricity Business Act, a pivotal policy initiative for energy liberalization (i.e., price deregulation) in Japan.

5.2.2 Trend interpolation

Complementing the UCSV model with the time-varying probability of zeros allows for better recovery of informative fluctuations in the trend, especially when there are informative asymmetries in the non-zero portion of observed inflation. Take, for example, *postage and*

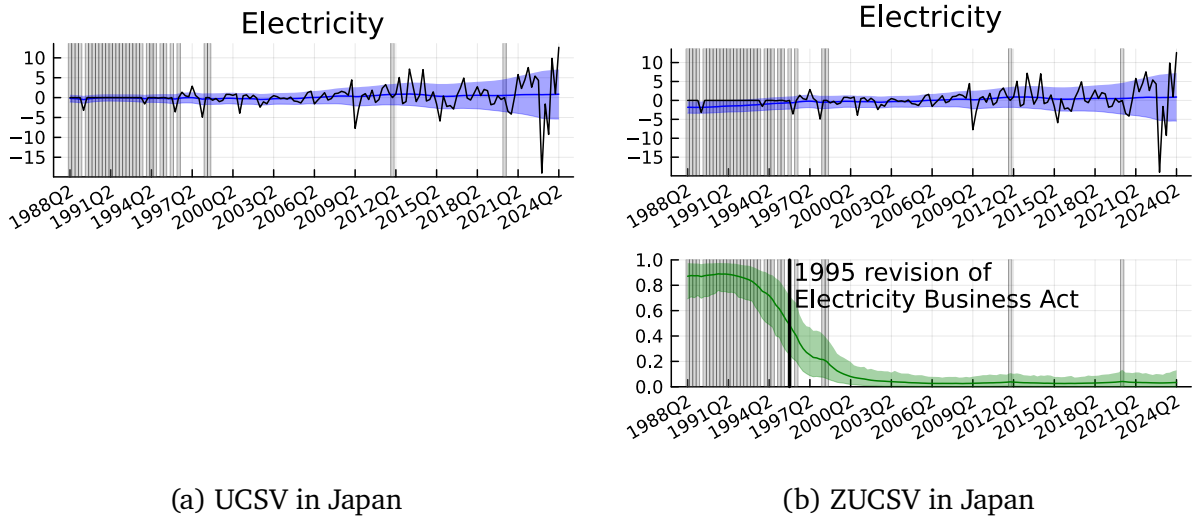


Figure 5: **Top:** Time-series plot of *electricity* inflation in Japan. The solid blue line represents the posterior mean estimate of the trend, while the shaded region indicates the posterior mean estimate of the time-varying volatility. **Bottom:** Posterior mean estimate of the time-varying probability of zeros. The shaded region represents the 90% credible interval.

delivery services in the US and *tutorial fees* in the UK, as shown in Figure [6]. Both have significant occurrences of zeros and almost exclusively non-negative observations. The multivariate ZUCSV model interpolates the latent trend(s) when the observations take zeros. The non-zero-inflated UCSV provides a mere dynamic summary of the central tendency, inevitably being shrunk towards zero when there are zeros, exhibiting uninformatively spiky latent trend estimates.

5.2.3 Volatility estimation

Posterior estimates of time-varying log-volatilities are essential for distinguishing whether observed variations are permanent or transitory. However, in the presence of persistent zeros, volatilities may not be accurately reflected in the data (see Section [2]), and the model should conservatively account for the limited information available about volatility. Figure [7] illustrates this with two components in Germany where zeros are prominent. Compared to UCSVs, Z-UCSVs estimate volatility to be higher and more uncertain, even interpolating these values during periods when only zeros are observed. In contrast, UCSVs produce overconfidently lower volatility estimates, as zeros are directly incorporated into the likelihood as if generated by a Normal measurement process. For

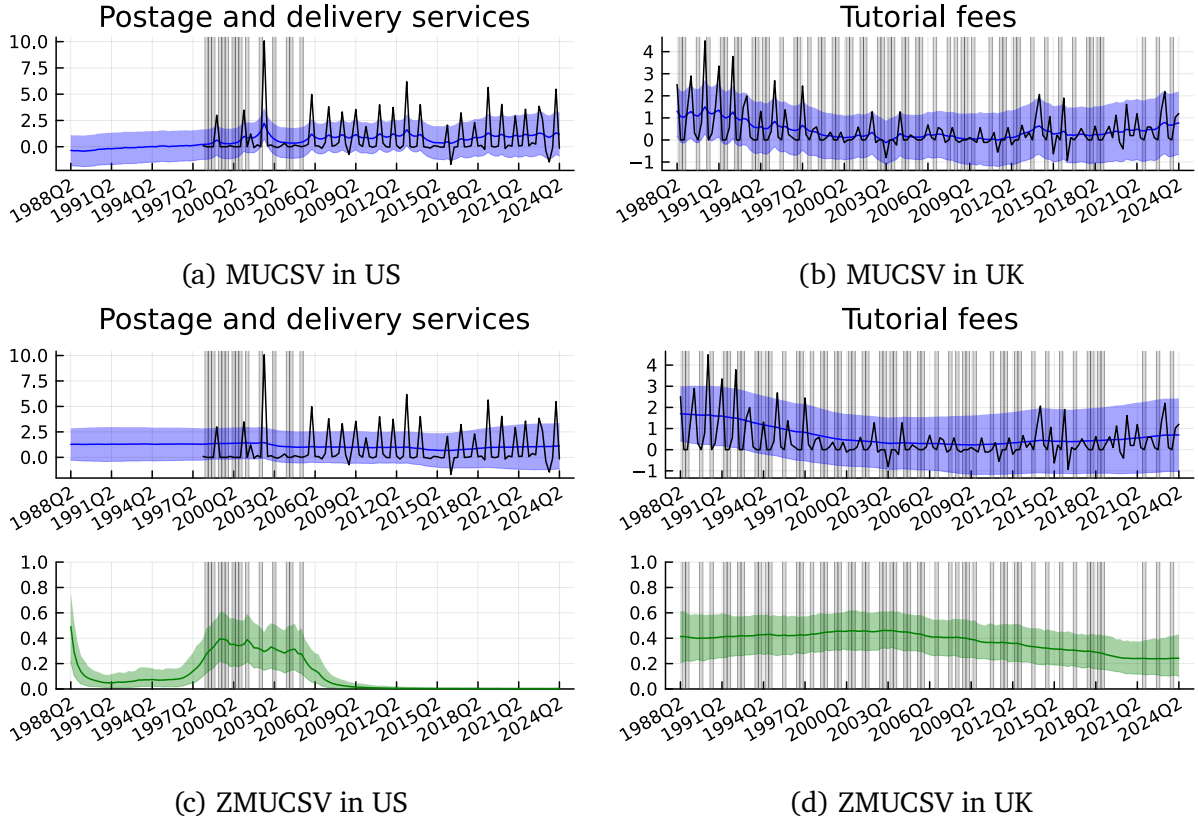


Figure 6: The solid blue line represents the posterior mean estimate of the trend, while the shaded blue region indicates the posterior mean estimate of the time-varying volatility. The solid green line represents the posterior mean estimate of the time-varying probability of zeros, and the shaded green region indicates the 90% credible interval.

components where zeros are (nearly) absent, the results are practically similar, with the posterior mass of the time-varying probabilities near zero. This underscores the utility of the zero-inflated model for handling components with substantial zero inflation while maintaining consistency for components without zeros.

5.2.4 Comovements

Figure [8] is a heatmap of the posterior mean of the covariance $\Sigma^{(\pi)}$ in Z-MUCSV. In US, there appears to be two clusters of indices that are interdependent to each other with regards to the evolution of the zero probability process. The former group tend to include specialized goods and services such as education and health services, whereas the latter group is composed primarily of tangible consumer goods and services such as apparel and footwear. Our model demonstrates sufficient flexibility to capture varying patterns of zero co-occurrence across the four countries analyzed.

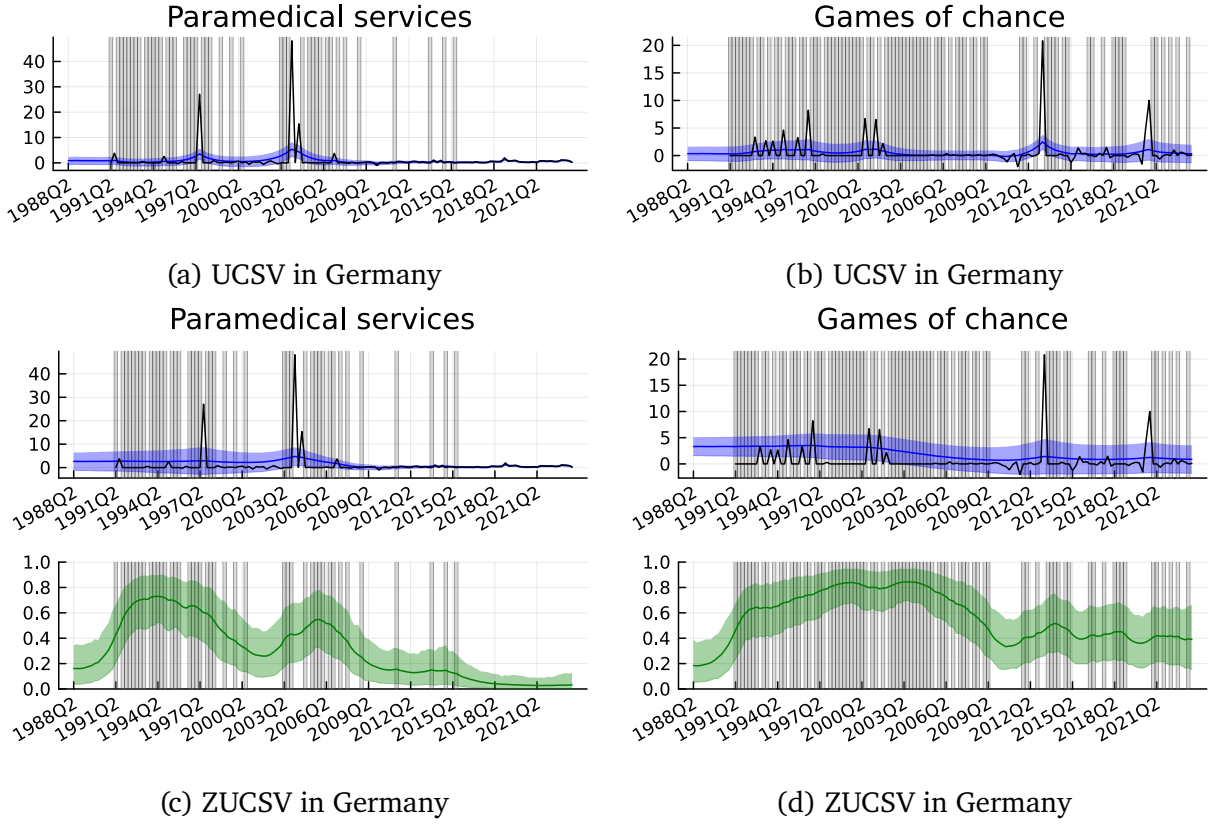


Figure 7: Solid blue line indicates the posterior mean estimate of the trend. Shaded blue region indicates the posterior mean estimate of the time-varying volatility. Solid green line indicates the posterior mean estimate of the time-varying probability of zero. Shaded green region indicates the 90% credible interval.

5.3 Out-of-sample forecasting exercise

5.3.1 Setup

We present results from a recursive out-of-sample forecasting exercise conducted as follows. We begin by designating a data window of the first 45 available quarters of post-processed data from 1988:Q2 to 1999:Q2 as the training set, and the subsequent $H = 8$ quarters starting from 1999:Q3 as the holdout validation set. Using the training set and its associated index set $[T]$, we approximate the h -quarter-ahead posterior predictive distribution via forwardly simulating the thinned MCMC samples of vector forecasts, $\mathbf{y}_{T+h|T}^{(r)}$ for $h \in [H]$ (with r indexing the r -th thinned MCMC sample).

Both point and interval forecasts are considered. As for point forecasts, we approximate the marginal posterior median. We approximate this by taking the empirical median of MCMC samples $(\mathbf{y}_{T+h|T}^{(r)})_{r=1}^R$, element-wise, given $h \in [H]$. The median provides an appropriate and tractable summary of the posterior predictive distribution, allowing for the

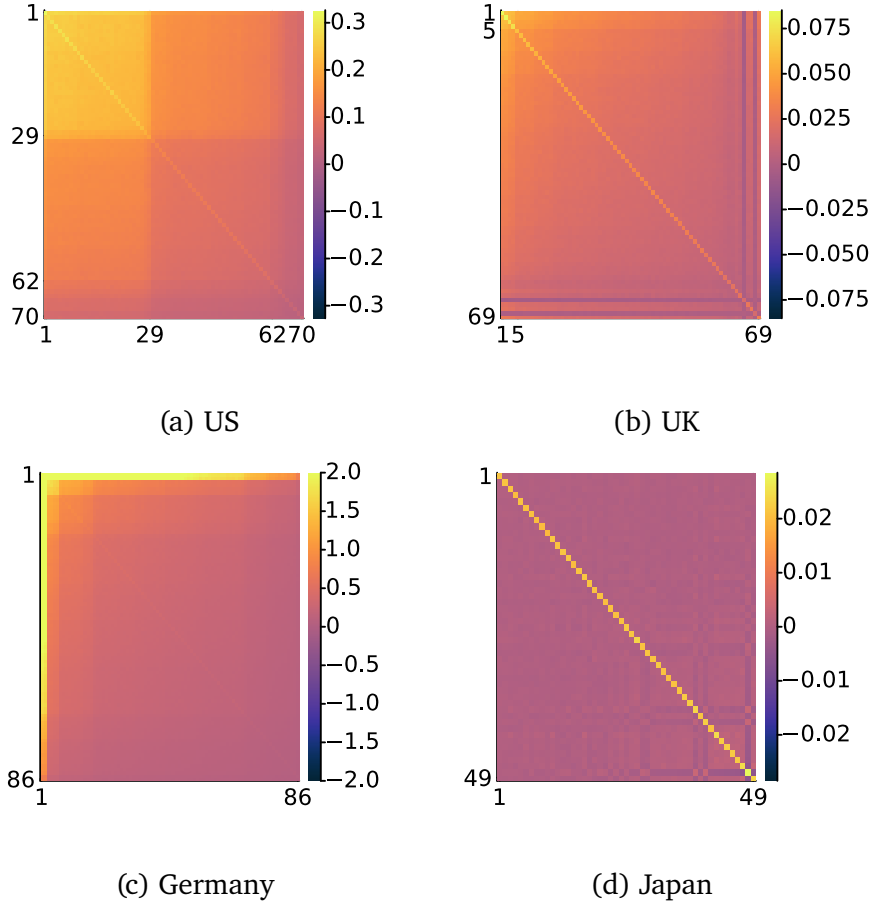


Figure 8: Posterior mean estimate of covariance of zero-probability evolution. **Note:** for a full list of component names, see the appendix.

forecast value to be exactly zero when warranted by the latent dynamic logistic sub-model, compared to the mean which is often employed as the default choice. Interval forecast is similarly approximated by an empirical central α -percentile interval.

Then, the next window of training samples with expanding window size (i.e., varying T) are used to compute the point forecast over the next holdout set. We repeat this until T is such that its $(H = 8)$ -quarters-ahead forecast corresponds to the final available data. In the final window, the holdout set ranges from 2020:Q3 to 2024:Q2, except for Germany, where the latest available disaggregated data was 2023:Q4 at the time we performed the analyses. We evaluate the out-of-sample point forecast performance with the empirical mean absolute error (MAE) relative to non-missing observations, and the interval forecasts by how well-calibrated over the distinct windows they are at different levels of α .

5.3.2 Point forecast

We have compared the one-quarter-ahead ($h = 1$) and eight-quarters-ahead ($h = 8$) forecast MAE values for all countries, components, and models. A complete set of visualizations is presented in the appendix to preserve space. For the majority of the components, all models exhibit similar performance in the sense that the within-component variability is smaller than the between-component variability. Note that all components were scaled to have equal empirical standard deviations prior to conducting posterior inference.

Important exceptions however are evident for some components in countries where zero-inflation is relevant: particularly in UK, Germany, and Japan. Figure [9] is the component-specific MAE of MUCSV relative to Z-MUCSV for short-term forecast horizons. A more detailed figure, as well as similar figures for long(er)-term horizons and univariate models is provided in the appendix. The results generally favor the zero-inflated model, as it provides improved point forecasts (a) on average compared to the non-zero-inflated model; we observe MAE improvements (i.e., decrements) with the zero-inflated model of approximately 0.21, 2.43, 2.98, and 4.84 percentage points, for US, UK, Germany, and Japan, respectively. In addition, (b) we observe improvements for a larger proportion of components across various country-horizon pairs. These underscore the utility of using the zero-inflated specification, which delivers superior forecast performance when zero-inflation is prevalent, while performing comparably to the non-zero-inflated model on average when zero-inflation is less prominent.

5.3.3 Interval forecast

Figure [10] shows the empirical coverage rates of interval forecasts for the multivariate models at various percentile levels, with rates computed over different forecast time points. Alignment with the 45-degree line (not shown) would indicate the ideal case in the frequentist sense where the $\alpha\%$ -central prediction interval covers $\alpha\%$ of the out-of-sample data. Given the high number of components, we have summarized the results by averaging the coverage rates at each $\alpha\%$ -central level. We note that *left-tails* for some calibration lines for the zero-inflated model is missing, as we have omitted regions where the prediction intervals have totally degenerated to $\{0\}$. Such regions only yield uninforma-

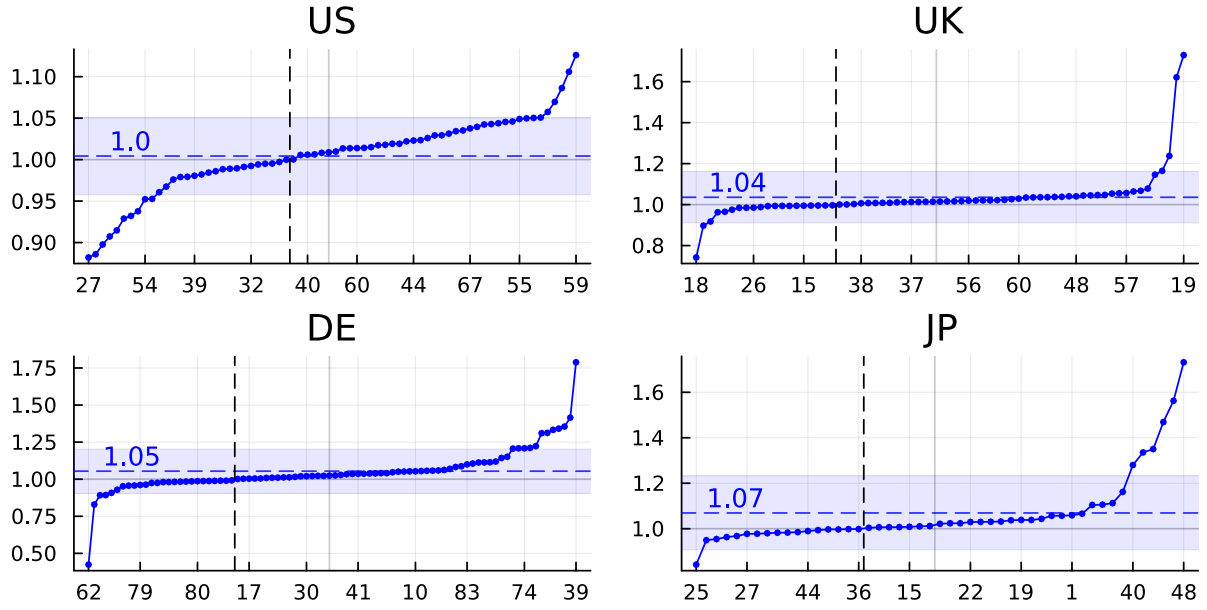


Figure 9: **Blue dots**: component specific empirical MAE ratio of MUCSV relative to Z-MUCSV, for $(h = 1)$ -quarter-ahead forecasts; higher values indicate that the point forecast was better for the zero-inflated model. **Blue dashed line**: average. **Blue shaded region**: two-standard-deviation band. **Black dotted line**: *break-even point*. **Note**: components have been ordered in ascending order. For plots with full annotations, see appendix.

tive and misleading summaries on the data about the proportion of zeros in the hold-out observations, given that we only have finite MCMC draws, which does not compare fairly to non-zero-inflated models without such abnormalities.

An immediate observation is that both multivariate models tend to exhibit over-coverage. However, the zero-inflated model consistently outperforms the non-zero-inflated model — whether univariate or multivariate — being closer to the 45-degree line on average. The improvement in calibration is particularly pronounced for countries with a higher prevalence of zeros in the disaggregated components (e.g., UK, Germany and Japan). In contrast, the difference is less evident for countries with fewer zeros (US), where both models perform similarly.

To investigate further, we decompose the interval forecast results by breaking down the plots into different *major* categories (see section 2.1 for data description). Figure [11] highlights the two major categories that exhibit substantial observable differences in the averaged calibration lines: health- and housing/water/fuels-related components (e.g., respectively including medical and sewage services). These items tend to undergo price

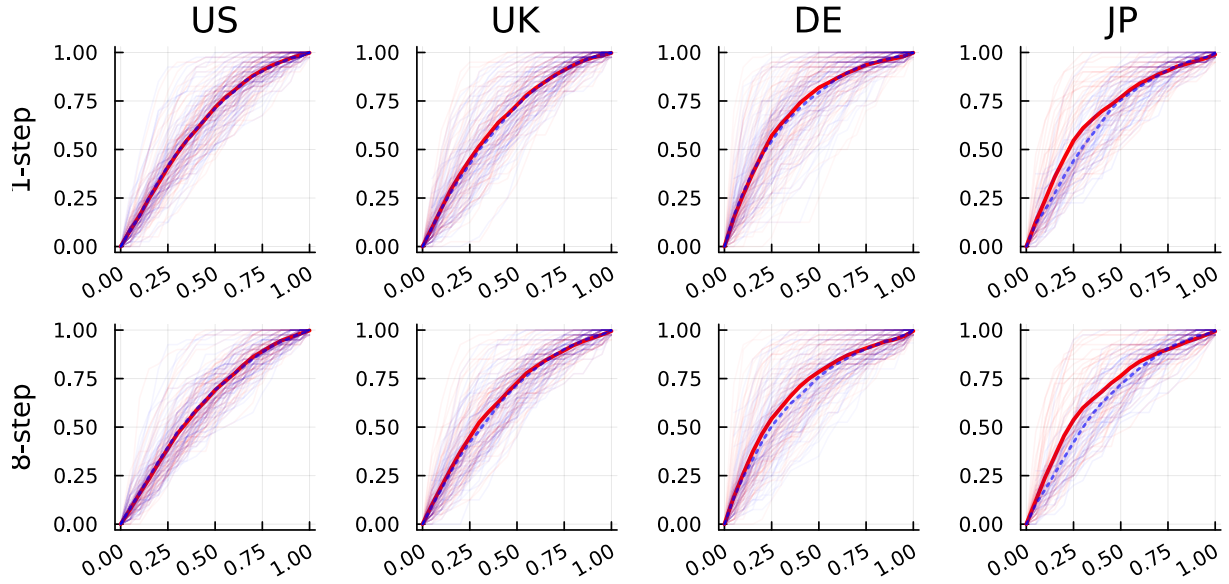


Figure 10: Empirical coverage (y-axis) of 1- and 8-quarter-ahead $\beta\%$ interval forecasts at different levels of β (x-axis) for the multivariate model, for each of the components in different countries; alignment to the 45-degree line (not shown) indicates perfect calibration. Average calibration performance is summarized by a **red solid line (MUCSV: non-zero-inflated)** and a **blue dotted line (ZMUCSV: zero-inflated)**.

revisions only after administrative processes, resulting in observable inflation occurring intermittently and contributing to the persistence of zeros (see section 2.3). No substantial differentials in the averaged calibration lines were observed in other major categories where zeros are not as prevalent (see appendix for figures).

These further support the use of the zero-inflated model, as it delivers better-calibrated interval forecasts on average in scenarios where zeros are prevalent, while maintaining comparable performance to the non-zero-inflated model when zeros are infrequent. Figures for the $h = 8$ case (i.e., long(er)-term forecasts) and figures comparing the univariate models in the appendix also exhibit similar patterns favoring the zero-inflated model.

6 Concluding remarks and future research

We introduced a novel zero-inflated stochastic volatility (SV) model that estimates the time-varying probability of exact zeros, leveraging the flexible framework of DGLMs. An efficient posterior Gibbs sampler, utilizing Pólya-Gamma augmentation, was developed to sample the time-varying probabilities effectively. Applying our model to a comprehensive

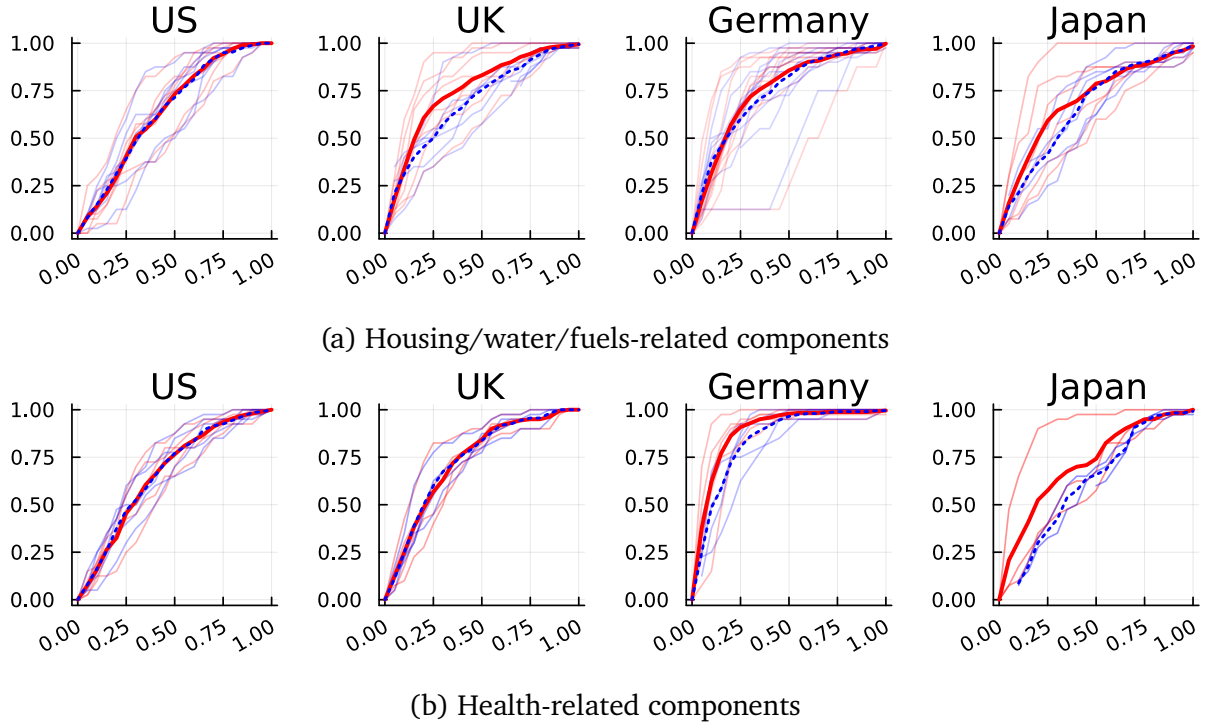


Figure 11: Empirical coverage (y-axis) of 1-quarter-ahead $\beta\%$ interval forecasts at different levels of β (x-axis) for selected components; alignment to the 45-degree line (not shown) indicates perfect calibration. Average calibration performance is summarized by a **red solid line (MUCSV: non-zero-inflated)** and a **blue dotted line (ZMUCSV: zero-inflated)**. **Note:** *left-tails* for some calibration lines for the zero-inflated model is missing as we have omitted regions where the prediction intervals have totally degenerated to $\{0\}$, to facilitate fair comparison with non-zero-inflated models.

dataset of disaggregated CPI inflation for the US, UK, Germany, and Japan, where zero-inflation was prevalent, we demonstrated that the zero-inflated model excels in capturing informative fluctuations in time-varying trends and volatility compared to traditional SV models, which often yield overly conservative estimates. In forecasting, the introduction of zero inflation improved performance across a larger number of disaggregated components and achieved better interval forecast coverage than the non-zero-inflated counterpart, particularly when zeros are prevalent.

We conclude by mentioning avenues for further research. A key unanswered substantive question is the extent to which price staleness contributes to aggregate inflation persistence (Cogley et al., 2010; Chan et al., 2016; Hwu and Kim, 2019) and how the Z-(M)UCSV model might quantify this relationship. An important methodological direction involves incorporating extensions of univariate (UC)SV models. Deterministic volatility feedback mechanisms have been explored in univariate (UC)SV models, such as those

in [Chan \(2017\)](#) and [Huber and Pfarrhofer \(2021\)](#), through stochastic volatility-in-mean models with time-varying parameters. These mechanisms could be incorporated alongside our proposed zero-inflated specification, and it would be worthwhile to empirically investigate whether such trend-volatility interactions exist in the context of disaggregated price inflation dynamics. Dynamic latent factor models ([Aguilar and West, 2000](#); [Lopes and Carvalho, 2007](#); [Negro and Otrok, 2008](#); [Gruber and West, 2016](#); [Lavine et al., 2022](#)) are widely used in macroeconomic and financial time-series to capture scalable, interpretable covariations. A pertinent question is how components cluster into factors and co-move with one another—a topic beyond the scope of this study, which focuses specifically on modeling zero-inflation. These directions offer promising avenues to enhance the understanding of price inflation processes. Extending the current framework to address these aspects remains a subject for future research.

Acknowledgments

We thank Mototsugu Shintani, Jouchi Nakajima, and Onishi Yuko for their helpful comments on the early version of this paper.

Funding

The second author’s research was partly supported by JSPS KAKENHI Grant Number 22K20132 from Japan Society for the Promotion of Science.

Disclosure Statement

The authors report that there are no competing interests to declare.

References

Aguilar, O. and West, M. (2000). Bayesian Dynamic Factor Models and Portfolio Allocation. *Journal of Business and Economic Statistics*, 18:338–357. [28](#)

- Albert, J. H. and Chib, S. (1993). Bayesian Analysis of Binary and Polychotomous Response Data. *Journal of the American Statistical Association*, 88(422):669–679. 14
- Barkan, O., Benchimol, J., Caspi, I., Cohen, E., Hammer, A., and Koenigstein, N. (2023). Forecasting CPI inflation components with Hierarchical Recurrent Neural Networks. *International Journal of Forecasting*, 39(3):1145–1162. 3
- Berry, L. R. and West, M. (2020). Bayesian Forecasting of Many Count-valued Time Series. *Journal of Business and Economic Statistics*, 38:872–887. 4, 10
- Bien, K., Nolte, I., and Pohlmeier, W. (2011). An Inflated Multivariate Integer Count Hurdle Model: An Application to Bid and Ask Quote Dynamics. *Journal of Applied Econometrics*, 26(4):669–707. 4
- Box, G. E. P., Jenkins, G. M., Reinsel, G. C., and Ljung, G. M. (2015). *Time Series Analysis: Forecasting and Control*. John Wiley and Sons Inc., 5 edition. 2
- Carter, C. K. and Kohn, R. (1994). On Gibbs sampling for State Space Models. *Biometrika*, 81(3):541–553. 13
- Chan, J. C. (2013). Moving Average Stochastic Volatility Models with Application to Inflation Forecast. *Journal of Econometrics*, 176(2):162–172. 3, 11, 12
- Chan, J. C. (2017). The Stochastic Volatility in Mean Model with Time-Varying Parameters: An Application to Inflation Modeling. *Journal of Business and Economic Statistics*, 35(1):17–28. 3, 28
- Chan, J. C. and Jeliazkov, I. (2009). Efficient Simulation and Integrated Likelihood Estimation in State Space Models. *International Journal of Mathematical Modelling and Numerical Optimisation*, 1(1–2):101–120. 14
- Chan, J. C., Koop, G., and Potter, S. M. (2013). A New Model of Trend Inflation. *Journal of Business and Economic Statistics*, 31(1):94–106. 3, 11
- Chan, J. C., Koop, G., and Potter, S. M. (2016). A Bounded Model of Time Variation in Trend Inflation, Nairu and the Phillips Curve. *Journal of Applied Econometrics*, 31(3):551–565. 3, 11, 27

- Chan, J. C. C., Koop, G., and Yu, X. (2024). Large Order-Invariant Bayesian VARs with Stochastic Volatility. *Journal of Business & Economic Statistics*, 42(2):825–837. 17
- Chib, S. (1992). Bayes Inference in the Tobit Censored Regression Model. *Journal of Econometrics*, 51(1):79–99. 3
- Cogley, T., Primiceri, G. E., and Sargent, T. J. (2010). Inflation-Gap Persistence in the US. *American Economic Journal: Macroeconomics*, 2(1):43–69. 11, 27
- Das, S. and Zhang, H. (2003). Rounding-up in reported EPS, behavioral thresholds, and earnings management. *Journal of Accounting and Economics*, 35(1):31–50. 15
- Dixon, H. D. and Grimme, C. (2022). State-dependent or time-dependent pricing? New evidence from a monthly firm-level survey: 1980–2017. *European Economic Review*, 150:104319. 3, 7
- Eo, Y., Uzeda, L., and Wong, B. (2023). Understanding Trend Inflation through the lens of the Goods and Services Sectors. *Journal of Applied Econometrics*, 38(5):751–766. 11, 17
- Faust, J. and Wright, J. H. (2013). Chapter 1 - Forecasting Inflation. In Elliott, G. and Timmermann, A., editors, *Handbook of Economic Forecasting*, volume 2 of *Handbook of Economic Forecasting*, pages 2–56. Elsevier. 3
- Frühwirth-Schnatter, S., Hosszejni, D., and Lopes, H. F. (2024). Sparse Bayesian Factor Analysis When the Number of Factors Is Unknown. *Bayesian Analysis*, pages 1–112. 17
- Frühwirth-Schnatter, S. (1994). Data Augmentation and Dynamic Linear Models. *Journal of Time Series Analysis*, 15(2):183–202. 13
- Frühwirth-Schnatter, S. and Frühwirth, R. (2007). Auxiliary Mixture Sampling with Applications to Logistic Models. *Computational Statistics & Data Analysis*, 51(7):3509–3528. 15
- Glynn, C., Tokdar, S. T., Howard, B., and Banks, D. L. (2019). Bayesian Analysis of Dynamic Linear Topic Models. *Bayesian Analysis*, 14(1):53–80. 4

- Gruber, L. F. and West, M. (2016). GPU-accelerated Bayesian Learning and Forecasting in Simultaneous Graphical Dynamic Linear Models. *Bayesian Analysis*, 11:125–149. 28
- Hausman, J. A., Lo, A. W., and MacKinlay, A. (1992). An Ordered Probit Analysis of Transaction Stock Prices. *Journal of Financial Economics*, 31(3):319–379. 4
- Hautsch, N., Malec, P., and Schienle, M. (2013). Capturing the zero: A new class of zero-augmented distributions and multiplicative error processes. *Journal of Financial Econometrics*, 12(1):89–121. 2
- Held, L. and Holmes, C. C. (2006). Bayesian Auxiliary Variable Models for Binary and Multinomial Regression. *Bayesian Analysis*, 1(1):145–168. 14
- Higo, M. and Saita, Y. (2007). Price Setting in Japan: Evidence from CPI Micro Data. Bank of Japan Working Paper Series 07-E-20, Bank of Japan. 7
- Huber, F. and Pfarrhofer, M. (2021). Dynamic Shrinkage in Time-Varying Parameter Stochastic Volatility in Mean Models. *Journal of Applied Econometrics*, 36(2):262–270. 3, 28
- Hwu, S. and Kim, C. (2019). Estimating Trend Inflation Based on Unobserved Components Model: Is It Correlated with the Inflation Gap? *Journal of Money, Credit and Banking*, 51(8):2305–2319. 3, 11, 27
- Kim, S., Shephard, N., and Chib, S. (1998). Stochastic Volatility: Likelihood Inference and Comparison with ARCH Models. *The Review of Economic Studies*, 65(3):361–393. 13
- Klenow, P. J. and Kryvtsov, O. (2008). State-Dependent or Time-Dependent Pricing: Does it Matter for Recent U.S. Inflation? *The Quarterly Journal of Economics*, 123(3):863–904. 3
- Kömm, H. and Küsters, U. (2015). Forecasting Zero-Inflated Price Changes with a Markov Switching Mixture Model for Autoregressive and Heteroscedastic Time Series. *International Journal of Forecasting*, 31(3):598–608. 2, 3

- Lavine, I., Cron, A. J., and West, M. (2022). Bayesian Computation in Dynamic Latent Factor Models. *Journal of Computational and Graphical Statistics*, 31:651–665. Published online December 30, 2021. 4, 28
- Levy, B. P. C. and Lopes, H. F. (2024). *Dynamic Ordering Learning in Multivariate Forecasting*, pages 81–109. Springer Nature Switzerland, Cham. 17
- Li, M. and Koopman, S. J. (2021). Unobserved Components with Stochastic Volatility: Simulation-based Estimation and Signal Extraction. *Journal of Applied Econometrics*, 36(5):614–627. 11
- Li, T. and Zheng, X. (2008). Semiparametric Bayesian Inference for Dynamic Tobit Panel Data Models with Unobserved Heterogeneity. *Journal of Applied Econometrics*, 23(6):699–728. 3
- Liu, L., Moon, H. R., and Schorfheide, F. (2023). Forecasting with a Panel Tobit Model. *Quantitative Economics*, 14(1):117–159. 3
- Lopes, H. F. and Carvalho, C. M. (2007). Factor Stochastic Volatility with Time Varying Loadings and Markov Switching Regimes. *Journal of Statistical Planning and Inference*, 137(10):3082–3091. Special Issue: Bayesian Inference for Stochastic Processes. 28
- Müller, H. (1987). A rasch model for continuous ratings. *Psychometrika*, 52(2):165–181. 15
- Nakajima, J. (2011). Time-Varying Parameter VAR Model with Stochastic Volatility: An Overview of Methodology and Empirical Applications. *Monetary and Economic Studies*, 29:107–142. 3
- Nakajima, J. and West, M. (2013a). Bayesian Analysis of Latent Threshold Dynamic Models. *Journal of Business and Economic Statistics*, 31:151–164. 3
- Nakajima, J. and West, M. (2013b). Bayesian Dynamic Factor Models: Latent Threshold Approach. *Journal of Financial Econometrics*, 11:116–153. 3
- Nakamura, E. and Steinsson, J. (2008). Five Facts about Prices: A Reevaluation of Menu Cost Models. *The Quarterly Journal of Economics*, 123(4):1415–1464. 3

- Neal, R. M. (2011). MCMC using Hamiltonian dynamics. In Brooks, S., Gelman, A., Jones, G., and Meng, X., editors, *Handbook of Markov Chain Monte Carlo*, chapter 5. Chapman and Hall/CRC. 15
- Negro, M. D. and Otrok, C. (2008). Dynamic Factor Models with Time-Varying Parameters: Measuring Changes in International Business Cycles. Staff Reports 326, Federal Reserve Bank of New York. 28
- Noel, Y. and Dauvier, B. (2007). A Beta Item Response Model for Continuous Bounded Responses. *Applied Psychological Measurement*, 31(1):47–73. 15
- Omori, Y., Chib, S., Shephard, N., and Nakajima, J. (2007). Stochastic Volatility with Leverage: Fast and Efficient Likelihood Inference. *Journal of Econometrics*, 140(2):425–449. 13
- Ospina, R. and Ferrari, S. L. (2012). A general class of zero-or-one inflated beta regression models. *Computational Statistics & Data Analysis*, 56(6):1609–1623. 15
- Polson, N. G., Scott, J. G., and Windle, J. (2013). Bayesian Inference for Logistic Models Using Pólya–Gamma Latent Variables. *Journal of the American Statistical Association*, 108(504):1339–1349. 4, 14
- Powell, B., Nason, G., Elliott, D., Mayhew, M., Davies, J., and Winton, J. (2017). Tracking and Modelling Prices using Web-Scraped Price Microdata: Towards Automated Daily Consumer Price Index Forecasting. *Journal of the Royal Statistical Society Series A: Statistics in Society*, 181(3):737–756. 3
- Primiceri, G. E. (2005). Time Varying Structural Vector Autoregressions and Monetary Policy. *The Review of Economic Studies*, 72(3):821–852. 3, 17
- Rydberg, T. H. and Shephard, N. (2003). Dynamics of Trade-by-trade Price Movements: Decomposition and Models. *Journal of Financial Econometrics*, 1:2–25. 4
- Stock, J. H. and Watson, M. (2016). Core Inflation and Trend Inflation. *The Review of Economics and Statistics*, 98(4):770–784. 11

- Stock, J. H. and Watson, M. W. (2007). Why has U.S. Inflation become Harder to Forecast? *Journal of Money, Credit and Banking*, 39(1):3–33. 3, 11, 13
- Sucarrat, G. and Grønneberg, S. (2020). Risk Estimation with a Time-Varying Probability of Zero Returns. *Journal of Financial Econometrics*, 20(2):278–309. 2
- Thomas, J. K. (1989). Unusual Patterns in Reported Earnings. *The Accounting Review*, 64(4):773–787. 15
- Wei, S. X. (1999). A Bayesian Approach to Dynamic Tobit Models. *Econometric Reviews*, 18(4):417–439. 3
- West, M. and Harrison, P. J. (1997). *Bayesian Forecasting and Dynamic Models*. Springer, 2nd edition. 2, 4, 12
- West, M., Harrison, P. J., and Migon, H. S. (1985). Dynamic Generalised Linear Models and Bayesian Forecasting (with discussion). *Journal of the American Statistical Association*, 80:73–97. 4, 12
- Windle, J., Carvalho, C. M., Scott, J. G., and Sun, L. (2013). Efficient Data Augmentation in Dynamic Models for Binary and Count Data. 4, 14
- Yanchenko, A. K., Deng, D. D., Li, J., Cron, A. J., and West, M. (2023). Hierarchical dynamic modelling for individualized Bayesian forecasting. *Journal of the Royal Statistical Society Series C: Applied Statistics*, 72(1):144–164. 4
- Zhang, B., Chan, J. C., and Cross, J. L. (2020). Stochastic Volatility Models with ARMA Innovations: An Application to G7 Inflation Forecasts. *International Journal of Forecasting*, 36(4):1318–1328. 3